NJC

Accepted Manuscript

This is an *Accepted Manuscript*, which has been through the Royal Society of Chemistry peer review process and has been accepted for publication.

Accepted Manuscripts are published online shortly after acceptance, before technical editing, formatting and proof reading. Using this free service, authors can make their results available to the community, in citable form, before we publish the edited article. We will replace this *Accepted Manuscript* with the edited and formatted *Advance Article* as soon as it is available.

You can find more information about *Accepted Manuscripts* in the Information for Authors.

Please note that technical editing may introduce minor changes to the text and/or graphics, which may alter content. The journal's standard Terms & Conditions and the Ethical guidelines still apply. In no event shall the Royal Society of Chemistry be held responsible for any errors or omissions in this *Accepted Manuscript* or any consequences arising from the use of any information it contains.

ROYAL SOCIETY OF CHEMISTRY

www.rsc.org/njc

Achieving Plasmon Reproducibility from Surfactant Free Gold Nanostar Synthesis

Jacob D. Ramsey[a], Lixia Zhou[a], C. Kyle Almlie[a], Jordan D. Lange[b], and Sean M. Burrows[,a]*

ABSTRACT

Obtaining reproducible plasmon resonances from nanostars remains a challenge for both surfactant and surfactant-free syntheses. For any nanostar application, a plasmon band with a reproducible spectral profile and λ_{max} is a fundamental criterion. In particular, synthesis of biocompatible gold nanostars will benefit from surfactant-free methods to alleviate concerns over the cytotoxicity of many surfactants used in current synthesis techniques and the relative ease of synthesis. In this paper, we analyze different surfactant-free nanostar synthesis conditions and their influence on achieving plasmon reproducibility. Plasmon reproducibility was judged via the standard deviation of the extinction spectra's λ_{max} and the spectral bandwidth. The synthesis temperature was the most influential factor in producing gold nanostars with reproducible plasmons. Nanostars synthesized at 5 °C exhibited a statistically ($\alpha = 0.05$) smaller standard deviation in both their λ_{max} and spectral bandwidth than nanostars synthesized at 25 °C. The reproducibility of the plasmon band was preserved even when the reaction conditions were adjusted to shift the position of the peak plasmon resonance. The high reproducibility of this approach, combined with the ease of synthesis, presents a significant step towards achieving gold

nanostars with reproducible plasmons for biological applications. For example, photodynamic therapy, biomedical imaging contrast agents, and biosensing will all benefit from the reproducibility of the nanostars plasmon bands.

KEYWORDS Plasmonics, Nanoparticles, Local Surface Plasmon Resonance, Temperature-Mediated/Surfactant-free Synthesis, Statistical Analysis, Electron Microscopy

INTRODUCTION

Nanostars are nanomaterials with spikes protruding from a spherical core. The sharp spikes facilitate strong Local Surface Plasmon Resonances (LSPRs) in the red to near infrared (NIR) spectral region. The strong LSPRs create a local electric field enhancement on the tip and between the sharp spikes on the individual stars as well as between the spikes of adjacent stars.[1–5] These attributes make them excellent tools in the emerging field of plasmonics.[6–8] The LSPR and near electric field enhancement result from the oscillation of conduction electrons interacting with light at the surface of the nanostar.[6] The peak plasmon resonance wavelength, referred to as λ_{max}, and electric field enhancement are heavily dependent on the size and shape of the particles and are often proportional to the length and aspect ratio of the spikes.[1,7–10] The spike length and aspect ratio influence the observed red shift of the nanostars plasmon away from the 520 nm peak of the gold nanosphere seed particles.[1] Additional electric field enhancement comes from the hybridization of plasmons from the spike tip and nanosphere core.[9] Hybridization of the plasmons from the various spike aspect ratios, as well as core and spike plasmon hybridization, give the nanostars plasmon resonance extinction spectrum a broad spectral profile. Typically, the Full Width Half Maximum of the spectrum extends over 150 nm.[1,11]

Biocompatible gold nanostars are of great value as their small size (30-60 nm) allows them to fit on and inside of cells.[1] Their unique optical properties make them excellent tools for analytical techniques and therapeutic applications, as gold nanoparticles have demonstrated reduced toxicity in human studies[1,12] For biological applications, a λ_{max} in the NIR is particularly useful. Compared to plasmon resonances excited at shorter wavelengths, NIR excitation allows for greater tissue penetration, reduced background from autofluorescence and light scatter, and causes less photothermal heat damage to the samples.[10,13] Gold nanostars have many potential applications such as medical diagnostics, biosensing, gyromagnetic imaging, photonic imaging, electronics, and others.[3,4,6,14,15] Each application could potentially require a different λ_{max}, which introduces a need for λ_{max} tunability. Additionally, for nanostars to be used as a reliable tool they require reproducible signals.[15–17]

The optical signal response is intrinsic to the nanostars geometric structure; however, the signal is usually an ensemble average from many nanostars. While it is virtually impossible to create nanostars with homogeneous structure, the average structure and collective signal needs to be reproducible for use as a reliable nanomaterial. There are some reports on the reproducibility of Surface Enhanced Raman Scattering signal for other types of nanoparticle geometries.[18–20] Often these reports were on the SERS reproducibility between a nanogap or of a single particle rather than focusing on the fundamental plasmon resonance from an ensemble of many particles. For these reasons, a synthesis technique is needed that produces nanostars with a reproducible plasmon resonance peak and spectral profile.

Many methods of nanostar synthesis exist, typically involving seed-mediated growth that begins with gold nanospheres as a substrate for growing the spikes to make star shapes.[1,6,16] Seedless methods also exist but are less common.[21,22] The nanostar growth mechanism is

strongly controlled by the local dielectric surroundings, and any small change to this can affect the synthesis.[4,23,24] Another factor that heavily influences the synthesis of the nanostars is the surface roughness of the nanosphere seed particles.[7,25] Surfactants such as Polyvinylpyrrolidone (PVP) or Cetyl Trimethylammonium Bromide (CTAB) are often used to mediate the growth of the spikes on the nanosphere surface.[11,13,21,22] These surfactants and others demonstrate cytotoxicity that limits their use in biological applications.[1,3,26] In some cases the complete post synthesis removal of these surfactants is very difficult to achieve.[1,27]

Biologically compatible nanostars using weakly interacting surfactants have been studied in-depth by the Pallavicini group.[27–30] These surfactants have been easily replaced post synthesis with thiol containing molecules and a centrifugal wash.[27,30] These methods of biocompatible gold nanostar synthesis have been successful, but they require longer reaction times and extra steps to replace surfactants with other surface coatings.[27,29] Additionally, some of the studies note the lack of monodispersity as three distinctly different morphologies were created from their synthesis procedures.[27,29] Work by others with surfactant-mediated approaches, and our own experiences with surfactant-free gold nanostar synthesis, revealed that each centrifugation step had the potential for loss of nanomaterial and increased potential for undesired aggregation.[1,14] For biological applications, the relative ease of synthesis and monodispersisty of the product in surfactant-free synthesis circumvents any potential issues associated with surfactant-mediated.[1,14,21]

Dey *et al*. and others remark that there is a lack of facile and robust procedures for synthesizing biocompatible gold nanostars that are both monodisperse and have reproducible plasmon resonances.[5,31,32] Reproducible plasmon resonances are needed for any application. For example, if λ_{max} and the plasmon band shape are not reproducible, then the Surface Enhanced

Resonant Raman signal can drastically change.[33] Thus, a reproducible surfactant-free method for nanostar synthesis is necessary for any application, especially those working in biological applications.[17,18]

According to work by Yuan *et al*., the nanostar growth in surfactant-free methods is controlled by Ascorbic Acid and Silver Nitrate ($AgNO_3$) concentration.[1] Previous methods have controlled growth via $HAuCl_4$ concentration.[7] Current understanding of this nanostar synthesis mechanism suggests that ascorbic acid reduces Au (III) to Au (0) on the gold nanosphere seed particle surface and the $AgNO_3$ concentration controls the anisotropic growth of the spikes.[1] Higher concentrations of $AgNO_3$ increase the spike length and surface coverage, directly controlling the λ_{max}.[1,13]

Following the surfactant-free gold nanostar synthesis of others we found it difficult to obtain reproducible plasmon band positions and profiles.[1] Variables such as pH and seed particle concentration have briefly been explored by Yuan *et al*.[1] They found that lowering the pH of the synthesis solution would lead to more red-shifted plasmon bands as would using fewer seed particles as it created larger nanostars.[1] The effect of temperature on nanostar λ_{max} position in a surfactant mediated synthesis technique was briefly addressed by Barbosa *et al*., but they only conducted experiments above room temperature.[6] Nucleation theory states that lower temperatures will decrease the activation energy and critical radius needed to initiate growth of the nanoparticles post nucleation. Additionally, the lower temperature will increase the number of stable nuclei but decrease the frequency of attachment of atoms in the liquid phase to the solid phase. These fundamental principles of nucleation provide a theoretical basis for low temperature synthesis influencing the geometric and plasmonic properties of nanostar synthesis.[34] To the best of our knowledge, a detailed study on the reproducibility of surfactant-free, seed

mediated gold nanostar plasmon resonance and the use of temperature, between 5 and 90 °C, to control reproducibility of the plasmon resonance has not been investigated.

Here we investigate the gold nanostar surfactant-free synthesis conditions that generate reproducible plasmon bands. Specifically, we were interested in the geometric shape, plasmon position, and plasmon reproducibility. Several synthesis conditions were evaluated in an attempt to achieve nanostars with a reproducible plasmon resonance in the NIR region. Here we explore pH, salt concentration, seed particle concentration, reaction time, and temperature as we follow the surfactant-free synthesis technique of Yuan *et al*.[1] Only the reaction temperature demonstrated sufficient control over the synthesis to give nanostars with reproducible plasmon resonances. The temperature controlled synthesis method has been developed along with adjustable $AgNO_3$ concentration as a significant step towards obtaining surfactant-free, biocompatible nanostars with plasmon resonances that are both tunable and reproducible. UV/Vis data were analyzed for statistical differences in the standard deviation of plasmon band positions and bandwidths. TEM images were analyzed to learn about the geometric shape of the nanostars at different synthesis temperatures.

EXPERIMENTAL

Materials and Instrumentation

Gold Chloride ($HAuCl_4$) Hydrate (Tetrachloroauric Acid) (99.999 %) was purchased from Sigma Aldrich, L-Ascorbic Acid (99.0 %), Hydrochloric acid (ACS grade), and Sodium Chloride (ACS grade) were purchased from Macron Chemical, Sodium Nitrate (ACS grade) and Nitric acid (ACS grade) were purchased from EMD, Sodium Citrate (99 %) was purchased from Acros, and Silver Nitrate (99.9 %) was purchased from Alfa Aesar. All reagents were used as received. All solutions were prepared using house de-ionized (DI) water. Gold seed particles were

synthesized according to the procedures described by Yuan *et al*.[1] Briefly, 15 mL of a 1% trisodium citrate solution was added to 100 mL of boiling 1 mM $HAuCl_4$ with vigorous stirring. Small additions of DI water to this solution kept the volume constant over the 15-minute reaction period. After cooling, the solution was filtered through a 0.22 μm nitrocellulose membrane (Corning, product # 430756). The gold seed solution was protected from light and kept at 4 °C for long-term storage.

Nanostars and seed solutions were characterized with UV/Vis spectrophotometry, Nanosight, and Transmission Electron Microscopy (TEM). A UV 1800 UV/Vis Shimadzu Spectrophotometer (Shimadzu, Kyoto, Japan) was used to obtain the nanostar spectral profiles. The following settings were used on the UV/Vis spectrophotometer: pitch-2.0 nm, Scan Speed-fast, Absorbance-0.000-2.000. A cell with a 1 cm pathlength was used for all UV/Vis measurements. Images of nanostars were obtained using a FEI Titan 80-200 TEM/STEM (FEI, Hillsboro, OR, USA, 80 kV or 200 kV). Concentration and average size information was obtained using a Nanosight NS 500 (Nanosight Ltd, Salisbury, UK).

Synthesis of Gold Nanostars at Different Temperatures

Biocompatible gold nanostars were synthesized using a modified surfactant-free procedure based on the techniques developed by Yuan *et al*.[1] Briefly, we doubled the volume of all reagents used in the synthesis in order to have enough material for characterization. 20 mL of 0.25 mM Gold Chloride was mixed with 20 μL of 1 M HCl and 200 μL of Gold Seed Particles (~ 12 nm) with moderate to vigorous stirring at about 800 rpm. For all reactions 100 μL of 100 mM Ascorbic Acid and 200 μL of a stock 3.0 mM $AgNO_3$ were added simultaneously with pipettes straight up and down as soon as possible after combining the first three reagents. For

nanostars synthesized above room temperature, beakers containing gold chloride, HCl, and gold seed particles were heated to the desired temperature. For synthesis below room temperature a water-ice bath was used. Once the desired temperature was reached, $AgNO_3$ and ascorbic acid were added to initiate the reaction. For the comparison of plasmon reproducibility under different $AgNO_3$ concentrations, we used 2.0 mM (S20 nanostars) and 3.5 mM (S35 nanostars) stock $AgNO_3$ instead of 3.0 mM $AgNO_3$ (S30 nanostars). The S20 and S35 nanostars also used 200 μL of their respective millimolar stock solution.

Unless otherwise stated, the nanostar reaction was allowed to proceed for 30 seconds. The reaction was quenched by centrifugation at 2000 rcf (relative centrifugal force) for 15 minutes. After centrifugation, the pellet was not completely solid and loss of material was a concern. To prevent loss of nanostar material, the supernatant was removed until only 2 mL remained. To disrupt aggregated particles, the samples were then sonicated for 8 minutes before filtering (0.22 μm nitrocellulose membrane). Filtering helps remove large or aggregated particles. The process of centrifugation was repeated twice after filtering. For these final centrifugation steps the supernatant was completely removed after each centrifugation, and the material was re-dispersed in 1 mL of DI water. Immediately following the final centrifugation, UV/Vis spectra were obtained for the samples.

Throughout the course of these experiments we found that multiple centrifugations reduced the yield and can lead to undesired aggregation. For optimal results we recommend only one additional centrifugation after quenching. After centrifugation the gold nanostars were condensed in a pellet at the bottom of the tube. If stored in this way the nanostars will aggregate and be rendered useless. It is essential to allow the nanostars to stay in pellet form for a minimal

time period to prevent aggregation at all steps. Samples were resuspended in DI water after centrifugation and kept at 4 °C for long-term storage.

All glassware and stir bars were washed with aqua regia (3:1, HCl:HNO_3) between uses. Proper safety precautions should be followed as HCl and HNO_3 are strong acids and HNO_3 is a strong oxidizing agent. Sodium Bicarbonate or alternative neutralizer should be used prior to disposal of acid waste.

Measurement of Nanostar Dimensions

The core diameter, tip-to-tip distance, spike length, and aspect ratio of nanostars were measured at 5, 25, and 40 °C using their respective TEM images in ImageJ software. At each temperature, five nanostars were analyzed. The core diameter and tip-to-tip distance were measured twice for each star. Four spikes on each nanostar were selected at random and measured as the length from the tip of the spike to its base defined by the edge of the core. One criterion for selection of a nanostar for measurement was that it could be visually well resolved from other nanostars. This limited the sample size we could measure. The aspect ratio of the spikes was determined using the length and width of the spikes. Because the width of the spikes changes along the length, we used the base width of the spikes.

Procedures for Determination of Au (III) to Au (0) Conversion Yield

To determine the conversion yield of Au (III) to Au (0) during synthesis of the nanostars at 5 and 25 °C, the UV/Vis peak of the gold chloride was monitored at 306 nm. The UV/Vis of just the gold chloride solution was taken before addition of gold seed solution, HCl, ascorbic acid, and $AgNO_3$. For each temperature, three replicate 20 mL aliquots of gold chloride were mixed

with HCl, ascorbic acid, and $AgNO_3$ for 30 seconds (as described above). To quench the synthesis, each replicate was separated into two 10 mL aliquots using 15 mL centrifuge tubes and centrifuged as described above. Immediately after the first centrifugation, the supernatant was sampled by removal of 8 mL from each vial and recombined (this was done for each replicate). The supernatant was then centrifuged again to make sure any nanostars carried over were pushed to bottom of centrifuge tube. Finally, UV/Vis analysis of the supernatant was used to determine the amount of gold chloride left over after the synthesis.

Solution Preparation for Aggregation Potential Study

Aggregation potential was determined from nanostars made at 5 and 25 °C by two of the authors, Jacob Ramsey (JR) and Lixia Zhou (LZ). Two authors were used to demonstrate trends between two different people making the nanostars. The concentrations of the nanostars made at each temperature by each author were determined with the Nanosight. After determining the concentration, each nanostar solution was brought to a concentration of 5×10^{10} nanostars/mL. These solutions were then used to prepare solutions containing a final concentration of 1×10^{10} nanostars/mL and 0, 15, 30, 75, and 150 mM NaCl.

RESULTS AND DISCUSSION

Reaction Conditions Influencing Gold Nanostar Synthesis

In general, synthesis of nanoparticles is difficult to reproduce and is heavily influenced by the local chemical and physical environment. Utilizing a surfactant-free nanostar synthesis technique, we attempted to obtain a reproducible λ_{max} in the NIR region.[1] Many factors were

explored with varying degrees of success. These factors included pH, salt concentration (ionic strength), seed particle concentration, reaction time, and temperature.

The pH, salt concentration, and seed particle concentration were only briefly explored because aggregation, lack of colloidal suspension, and lack of λ_{max} reproducibility prevented further analysis (data not shown). After centrifugation, the nanostars were concentrated in a pellet at the bottom of the centrifuge vial and were usually readily resuspend. However, studies into pH, salt concentration, and seed particle concentration often did not resuspend. The ionic strength of the reaction solution as described above was calculated to be 3.565 mM. We found changes in the ionic strength with NaCl and $NaNO_3$ by hundreds of micromolar or more influenced the morphology of the nanostars or caused them to aggregate. Even if the nanostars did not aggregate, the λ_{max} values were not reproducible. For solutions with decreased pH and lower concentrations of seed particle that did resuspend, red shifts further into the NIR region were observed. However, these changes significantly decreased nanostar yield as most of the nanostars spontaneously aggregated and did not readily suspend in solution. Due to aggregation of a majority of the nanostars, the samples were rendered useless.

Effect of Nanostar Synthesis Temperature on Plasmon Resonance Position and Reproducibility

The effect of temperature on the synthesis of gold nanostars has been studied for methods using surfactants at temperatures above room temperature (25 °C).[6] Here we investigated temperature effects on surfactant-free nanostar synthesis both above and below 25 °C. The

results of surfactant mediated synthesis techniques do not directly match those of the surfactant-free methods we performed and cannot be extrapolated to this study.

The effect of temperature on nanostar synthesis was investigated at 0, 5, 25, 40, 50, and 90 °C. UV/Vis spectra and Transmission Electron Microscopy (TEM) images were used to determine temperature effects on the nanostars optical properties and physical appearance, respectively. To gauge the reproducibility of the synthesis at different temperatures the standard deviation of the λ_{max} position and spectral width at three quarters full maximum were used. Full width half maximum was not used because some of the nanostars absorbed and scattered light near the upper limit of the spectrophotometers wavelength range (1000 nm).

Figures 1(a) and 2 demonstrate that at 5 °C a reproducible plasmon band was observed with an average λ_{max} of 751 nm and a standard deviation of ± 4 nm (n = 4, ~ 0.5 %relative standard deviation, RSD). The spectral width at three quarters full maximum ranged from 164 nm to 182 nm and averaged at 174 ± 8 nm (n = 4, ~ 5 % RSD). Synthesis at room temperature (25 °C) gave an average λ_{max} of 818 nm, but varied greatly with a standard deviation of ± 39 nm (n = 4, ~ 5 % RSD) (Figures 1(b) and 2). At 25 °C the width of the spectral profile at three quarters full maximum ranged from 202 to 338 nm and averaged about 254 ± 60 nm (n = 4, ~ 24 % RSD). The standard deviation of the λ_{max} (Figure 2) and peak width for nanostars synthesized at 5 °C were found to be significantly smaller (F-test, $\alpha = 0.05$), than those of nanostars synthesized at 25 °C. The smaller standard deviation in plasmon position and spectral width at 5 °C compared to 25 °C support the argument that nanostars made at 5 °C were more reproducible than those made at 25 °C. Trials 1-3 used the same stock solutions of gold chloride, gold seed particles, ascorbic acid, and $AgNO_3$. Trial 4 used a different batch of stock reagents and was conducted a week later to ensure and give more confidence to the reproducibility at 5 °C.

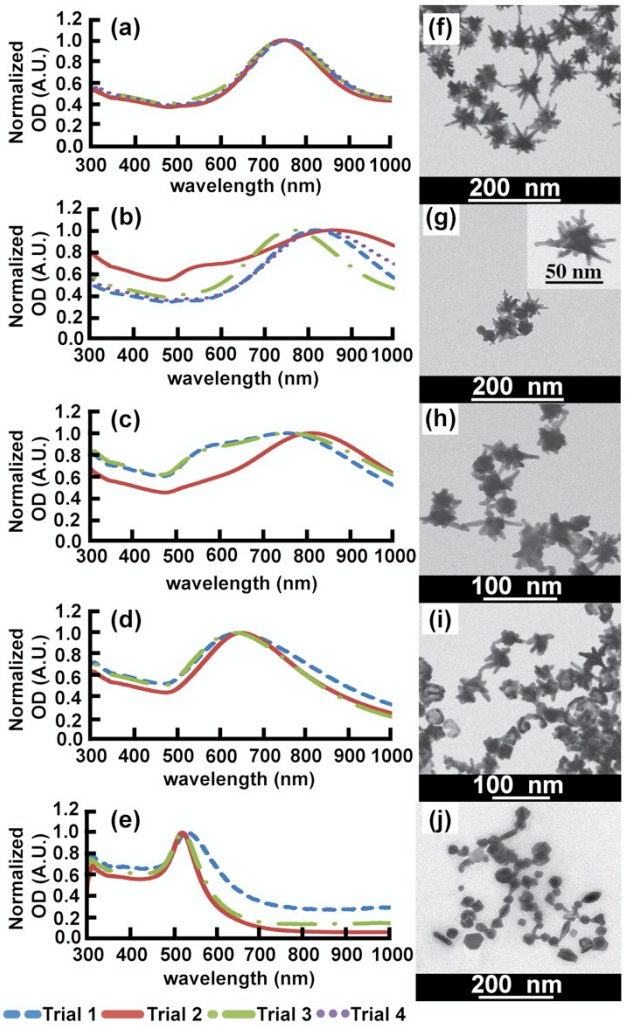

Figure 1. Normalized optical density (OD) showing the reproducibility of the plasmon resonance bands and TEM images showing the morphology of the gold nanostars when prepared at different temperatures: (a, f) 5 °C, (b, g) 25 °C, (c, h) 40 °C, (d, i) 50 °C, and (e, j) 90 °C. All experiments were conducted in triplicate except for 5 °C and 25 °C with n = 4. Notice 1a for 5 °C has better reproducibility in terms of plasmon peak position and spectral width at three quarters full maximum than the other temperatures.

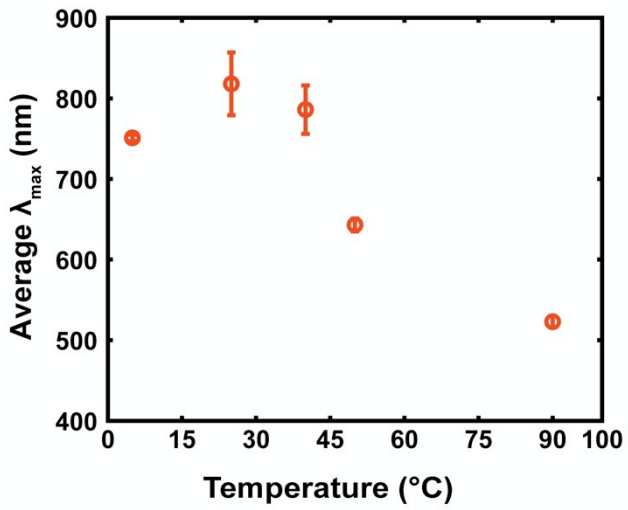

Figure 2. Average and Standard Deviation of the peak plasmon resonance wavelength (λ_{max}) from nanostars synthesized at different temperatures (n = 3, except for the nanostars at 5 and 25 °C with n = 4). The 5 °C has the lowest error out of all the synthesis temperatures. Error bars represent ± one standard deviation unit; some error bars are the same size or smaller than the symbol.

To further explore the nature of the plasmon reproducibility we examined the length of the spikes protruding from the gold nanosphere core. From the TEM images in Figure 1 and some that were not shown, the core diameter, spike length, tip-to-tip distance, and aspect ratio were measured as described in the experimental. The cores of the nanostars made at 5 and 25 °C were statistically similar in both the average and standard deviation: 31.0 ± 3.0 nm (n = 10) and 33.0 ± 5.0 nm (n = 10), respectively. The nanostars made at 5 °C had long spikes with an average length of about 28.5 ± 7.9 nm (n = 20) as seen in Figure 1(f). These spikes were statistically longer ($\alpha = 0.05$) than the spikes on the 25 °C nanostars (21.8 ± 9.2 nm (n = 20)). The inset of Figure 1(g) shows that nanostars made at 25 °C also had side branches. The tip-to-tip distance of the nanostars is a critical feature for biomedical applications as they give vital information about

the size of the particles and thus their usefulness in biological environments. When synthesized at 5 °C and 25 °C, the average tip-to-tip distances were 81.9 ± 8.2 nm (n = 10) and 72.8 ± 20.5 nm (n = 10), respectively. The standard deviation of the tip-to-tip distance was statistically smaller at 5 °C than 25 °C ($\alpha = 0.05$). The aspect ratio $\left(\frac{Spike\ Length}{Spike\ Width}\right)$ of the spikes is integral to the plasmon band position. The average aspect ratio for nanostars synthesized at 5 °C was 2.58 ± 0.89 (n = 32). Those synthesized at 25 °C had an average aspect ratio of 3.35 ± 1.12 (n = 11). The aspect ratio was statistically smaller ($\alpha = 0.05$) in the nanostars made at 5 °C than those at 25 °C. The differences in aspect ratio likely play a key role in the plasmon peak position differences between the nanostars made at different temperatures. The lower standard deviation in the tip-to-tip distance of the nanostars synthesized at 5 °C was suspected to contribute to the reproducible λ_{max} position, spectral shape, and spectral width.

Figures 1(c) and 2 show that the nanostars made at 40 °C had an average λ_{max} of 786 nm and a large standard deviation of ± 30 nm (n = 3). The average spectral width at 40 °C was about 353 ± 72 nm (n = 3) and varied from 272 nm to 410 nm. The large standard deviation of the λ_{max} and spectral width show that the nanostars synthesized at 40 °C were not reproducible. The approximately 20 % variability in the width of the spectral profile was a result of the heterogeneity of the shapes produced. Figure 1(h) reveals that some of the nanostars had just one or two spikes off the core. Of the spikes that could be measured, the average length was 17.5 ± 7.4 nm (n = 20) and was not statistically different from the spikes exhibited by the nanostars synthesized at 25 °C, but statistically smaller than those made at 5 °C ($\alpha = 0.05$). The nanostar core diameters and tip-to-tip distances from the 40 °C synthesis were 23.8 ± 5.3 nm (n = 10) and 53.9 ± 15.4 nm (n = 10), respectively. The average core diameters and tip-to-tip distances were statistically smaller than those of both the 5 and 25 °C syntheses. The standard

deviation of the tip-to-tip distance for the nanostars made at 40 °C was statistically larger than that of the nanostars made at 5 °C.

As the temperature increased past 40 °C the plasmon continued to blue shift (with respect to synthesis at 25 °C) and various shapes of nanoparticles were formed. Figures 1(d) and 2 show the nanoparticles made at 50 °C exhibit an average λ_{max} of 643 nm corresponding to a blue shift of about 175 nm. Figure 1(i) shows the material produced from synthesis at 50 °C was a mixture of nanostars and other nanoparticle geometries. Figure 1(j) for synthesis at 90 °C shows that many more nanoparticle geometries were produced (nanorods, nanospheres, nanocubes etc.). Figure 3 shows that the nanomaterial synthesized at 90 °C had a λ_{max} near 523 nm and was very similar to that of the gold seed particle solution.

From Figures 1(d), 1(e), and 2 for 50 and 90 °C, the standard deviations (n = 3) were lower at ± 8 and ± 7 nm, respectively. While the λ_{max} position was reproducible for both 50 and 90 °C, the spectral shapes and widths were not very reproducible (Figure 1(d) and 1(e)). At 50 °C the spectral widths ranged from 186 nm to 238 nm and gave an average width of 211 ± 26 nm (n = 3, 12 % RSD). The width for the 90 °C reaction ranged from 54 nm to 96 nm and averaged at 71 ± 22 nm (n = 3) with a 31 % RSD. The variation in peak shape and width was most likely due to the mixture of nanostars and other nanoparticle geometries present at these higher synthesis temperatures.

As the reaction temperature increased past 40 °C the pink gold chloride solution containing seed particles gradually became clearer. However, as the temperature increased past 70 °C, the solution gradually became pinker again. At both 50 and 90 °C, the reaction appeared to finish within a second. The 50 °C reaction occurred as expected, producing a solution with a dark blue-grey/green tint. In the 90 °C reaction, upon addition of the ascorbic acid and the $AgNO_3$, a

dark pink/purple color was observed. The observed colors correlated well with the observed plasmon λ_{max} values of 643 nm and 523 nm at 50 °C and 90 °C, respectively. After centrifugation, the 50 °C had a slightly blue colored supernatant, but the 90 °C reaction had a slightly pink supernatant. The 90 °C reaction had a pellet that appeared pink and dark blue.

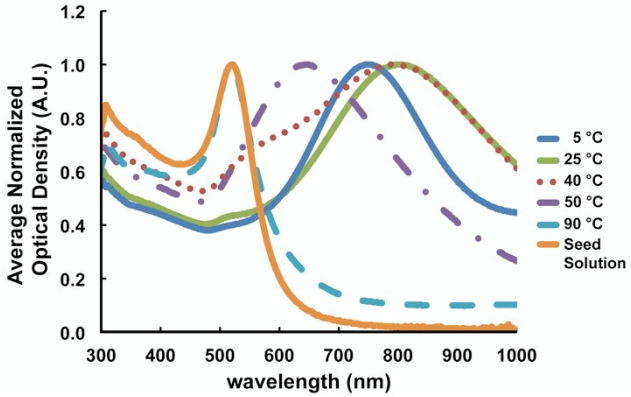

Figure 3. Average normalized optical density of plasmon bands from nanomaterial synthesized at each temperature as well as that of the seed solution (gold nanospheres). Notice the plasmon peak red shifts from the seed solution with addition of $AgNO_3$ and ascorbic acid. The extent of the red shift depended on temperature with the 25 °C synthesis temperature showing the greatest red shift.

To summarize the data so far, synthesis at 5 °C gave nanostars with the best reproducibility in terms of standard deviation of the plasmon peak position (λ_{max}), spectral width, and tip-to-tip distance (Figures 1, 2, and 3). While the 25 °C synthesis yielded nanostars, the λ_{max}, spectral width, and tip-to-tip distance were not reproducible. At temperatures between 40 °C and 90 °C, a mixture of gold nanostars and many kinds of nanoparticles were produced. The nanostars at 40 °C and 50 °C did not have very well defined spikes and often contained other nanoparticle geometries. No nanostars were observed at 90 °C. Instead, a variety of nanoparticle geometries were made. Figure 2 helps summarize the data according to reproducibility of the average and

standard deviation of the plasmon λ_{max}. Figure 3 demonstrates the effect of the nanostars λ_{max} position and spectral profile as a function of temperature and how the λ_{max} of the nanostars related to that of the seed solution. Formation of nanostars caused a red shift in the plasmon resonance with respect to the seed solution. As the temperature changes from 25 °C, the nanostar λ_{max} blue shifts back toward that of the seed solution. The remainder of the discussion will focus on 5 and 25 °C syntheses because those temperatures yielded more nanostars than the other temperatures.

Au (III) to Au (0) Conversion Yield

The extinction peak at 306 nm from gold chloride was monitored before and after nanostar synthesis to determine the conversion yield of Au (III) to Au (0) (see experimental for more detail on the procedure). The conversion yield for synthesis at 5 °C and 25 °C were 92.1 ± 2.1 % (n = 3) and 89.5 ± 1.4 % (n = 3), respectively. These differences were not significantly different ($\alpha = 0.05$).

Tuning Plasmon Resonance with the $AgNO_3$ *Concentration at 5 and 25 °C*

Nanostars exhibit λ_{max} values in the NIR region and are thus highly valuable in a variety of biological applications. Depending on the particular biological application or light source used, different λ_{max} values may be needed. Adjusting the $AgNO_3$ concentration has been shown to tune the λ_{max} to desired values.[1] The 5 °C synthesis was tested at different $AgNO_3$ concentrations to see if the plasmon band could still be tuned and maintain reproducibility when compared to the 25 °C synthesis.

All the data presented so far used a final concentration of 30 μM $AgNO_3$ in the reaction vessel. We will now use the nomenclature S30 to refer to nanostars made using a final $AgNO_3$ concentration of 30 μM, S20 to refer to a final $AgNO_3$ concentration of 20 μM, and S35 to refer to a final $AgNO_3$ concentration of 35 μM. As seen in Figure 4 and Figure S1, adjusting the $AgNO_3$ concentration under 5 °C synthesis conditions still allowed tuning of the plasmon band to a desired λ_{max} position. Use of 20 μM $AgNO_3$ in the reaction yielded nanostars with a plasmon band at 671 ± 6 nm (n = 3) when synthesized at 5 °C. The plasmon λ_{max} had a statistically smaller standard deviation for the S20 nanostars made at 5 °C compared to the standard deviation of ± 41 nm (n = 3) for S20 nanostars synthesized at room temperature (F-Test, α = 0.05).

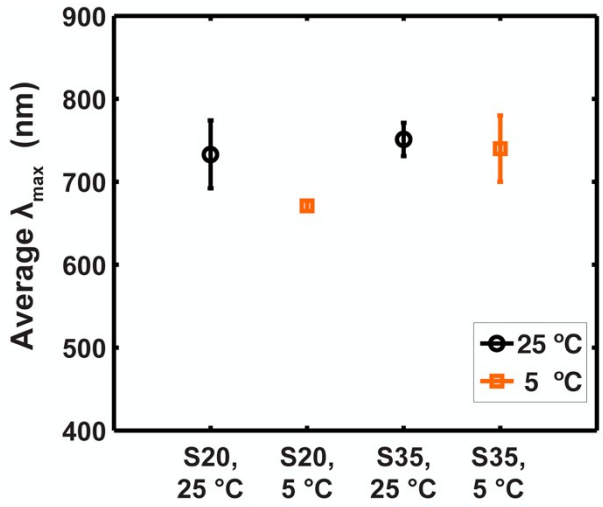

Figure 4. Average plasmon λ_{max} of nanostars made at different $AgNO_3$ concentrations and temperatures. S20 (n = 3) nanostars used 20 μM $AgNO_3$ for synthesis and S35 (n = 3) used 35 μM $AgNO_3$ for synthesis (all concentrations were the final concentration in reaction vessel). Synthesis of S20 nanostars at a reaction temperature of 5 °C gave a statistically smaller (α = 0.05) standard deviation in the λ_{max}, by a factor of 6.5, than S20s made at room temperature. The standard deviation of the λ_{max} for S35s made at 5 °C was not statistically different from that of

the room temperature (F-test, $\alpha = 0.05$). Therefore, both the S35s made at room temperature and at 5 °C were not very reproducible. The error bar for the S20s at 5 °C were the same size or smaller than the symbol, error bars represent ± one standard deviation unit.

No further red shift in the λ_{max} with respect to seed solution was observed after adding $AgNO_3$ with a concentration greater than 30 μM (Figures 4 and Figure S1). Instead the average λ_{max} of nanostars with 35 μM $AgNO_3$ appeared to blue shift with respect to S30s, but the average λ_{max} was not reproducible and the extent of blue shift could not be precisely determined due to the large standard deviation (Figure 4 and Figure S1 of supporting information). We found no statistical difference ($\alpha = 0.05$) from an F-test comparing the standard deviations of S35 nanostars at room temperature to those at 5 °C. Therefore, neither the synthesis of S35s at room temperature nor at 5 °C gave very reproducible plasmons.

Work by Fales *et al*. showed that gold nanostars coated with silver caused a significant blue shift with additional aliquots of $AgNO_3$.[13] If excess silver exists after the nanostar synthesis was complete, then it may have formed a silver coating. If a silver coating did form, then this would provide an explanation for the apparent blue shift in the plasmon band of the S35 nanostars relative to the plasmon band of S30 nanostars. A blue shift from a silver coating would be expected as silver nanoparticles have λ_{max} values near 425 nm.

Figures 5(a) and (b) show TEM images of the S20 nanostars at 25 °C and 5 °C, respectively. The tip-to-tip distance of the S20s at each temperature were about 60 nm and had about 35 nm cores. For both temperatures, the spikes of S30s were easier to see than those of the S20s (compare Figures 5(a) and (b) to Figures 1(f) and (g))

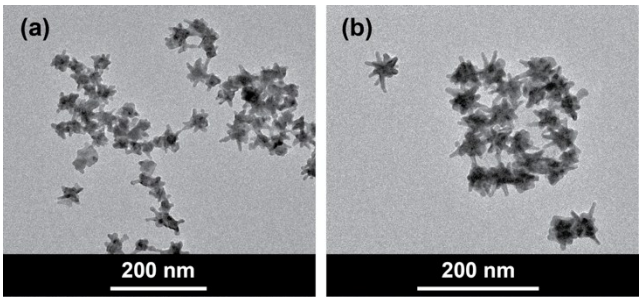

Figure 5. TEM image of S20 nanostars at (a) 25 °C and (b) 5 °C. The S20s at each temperature were about 60 nm tip-to-tip and had about 35 nm cores.

Gold Nanostar Stability and Susceptibility to Aggregation

The stability over time for the nanostars made at 5 °C was studied in DI water. Over the span of 21 days the λ_{max} dropped from 737 nm to 699 nm (data not shown). After 21 days, the nanostars aggregated and crashed out of solution, rendering them useless. Because of this limited stability, nanostars are best used within a few weeks of synthesis and stored in DI water.

For the gold nanostars to function as an analytical tool, they need to be stable and resist aggregation in solution. The aggregation state of the nanostars is heavily influenced by the ionic strength of the solution. Even small changes to the local ionic environment of the nanostars will cause significant changes in the nanostar aggregation state.

The susceptibility of nanostars to aggregation was studied by changing the NaCl salt concentration in a method adapted from the work of Levy *et al*.[35] Two of the authors, Jacob Ramsey (JR) and Lixia Zhou (LZ), each synthesized nanostars at 5 °C and 25 °C. After synthesis, all nanostar solutions were adjusted to 1 x 10^{10} nanostars/mL with increasing NaCl concentrations of 0, 15, 30, 75, and 150 mM.

Aggregation Potential was measured using the peak optical density (OD) ratio (Equation 1) and shift in the peak plasmon wavelength, $\Delta\lambda_{max}$ (Equation 2). The 'x M NaCl' in equations 1 and 2 corresponds to the different salt concentrations investigated (0 to 150 mM NaCl).

$$\text{OD ratio} = \frac{\text{OD}_{\text{max}}(0\text{ M NaCl}) - \text{OD}_{\text{max}}(\text{x M NaCl})}{\text{OD}_{\text{max}}(0\text{ M NaCl})} \quad (1)$$

$$\Delta\lambda_{max} = \lambda_{\text{max}}(0\text{ M NaCl}) - \lambda_{\text{max}}(\text{x M NaCl}) \quad (2)$$

An aggregation potential of zero for either metric indicated no aggregation. Deviations from zero represent a change in the aggregation state of the nanostars. Figure 6 (a) and (b) show that the nanostars aggregated as the salt concentration was increased. For nanostars made at 5 and 25 °C, the aggregation potentially steadily increased from 0 to 30 mM NaCl. At 75 mM and beyond the aggregation potential plateaued. From range finding experiments to determine NaCl concentrations to use (data not shown), we found all solutions visibly changed color from a dark green/blue hue to a more clear blue hue at 50 mM NaCl.

The aggregation potential of the nanostars made at 5 and 25 °C behaved differently when looking at both the peak optical density ratio and plasmon λ_{max} shift. For nanostars prepared by each author (JR and LZ), as the salt concentration increased, the aggregation potential increased faster for the nanostars made at 25 °C than the 5 °C. This effect was much more noticeable when looking at the $\Delta\ \lambda_{max}$ rather than the OD ratio. Since each author (JR and LZ) independently made the same observation regarding the aggregation potential, we concluded that nanostars made at 5 °C were less susceptible to aggregation than the nanostars made at 25 °C for salt concentrations less than 75 mM.

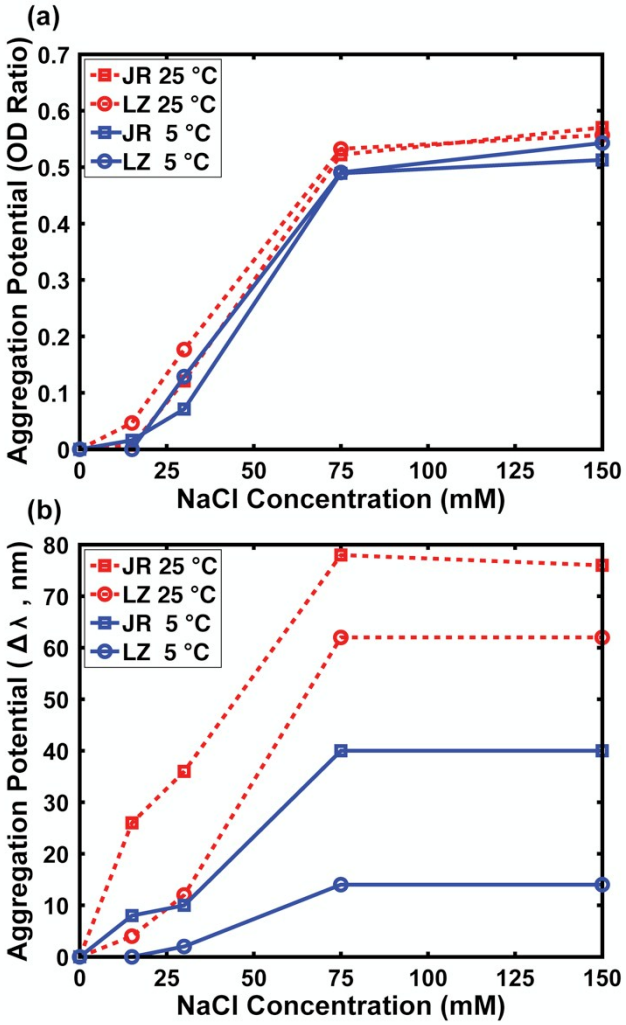

Figure 6. Aggregation potential of nanostars made at 5 and 25 °C. Trials were performed by two of the authors (Jacob Ramsey (JR) and Lixia Zhou (LZ)) and similar trends were observed from nanostars prepared by both authors. The gold nanostar aggregation potential as (a) the peak optical density ratio and (b) the shift in plasmon λ_{max}, ($\Delta\lambda_{max}$) vs. NaCl concentration (0, 15, 30, 75, and 150 mM). Below 75 mM NaCl, nanostars made at 5 °C demonstrated less potential for aggregation than those made at 25 °C (compare nanostars made by each author at the two temperatures).

Investigation of Reaction Time at 5 °C

According to one study done by Yuan *et al*., the reaction at room temperature was complete within 30 seconds after the addition of Ascorbic Acid and $AgNO_3$.[1] We observed that as the reaction occurred at 25 °C, the color changed from light pink to a dark blue-gray over 3 - 5 seconds. At 5 °C, the solution started out a light pink and then slowly turned to a light gray, then to a dark gray, and then to a deep blue-gray. This color change took 10 - 30 seconds, indicating that the reaction may take longer to complete at lower temperatures. We suspected that the lower temperature might slow down reduction of gold onto the nanosphere surface allowing for a more controlled, reproducible growth of the spikes. At 5 °C we hypothesized that if the reaction does not complete in 30 seconds, then the λ_{max} should shift relative to the 30 second time point as more gold gets deposited onto the nanospheres at longer reaction times.

To test this hypothesis a time study at 5 °C was performed. We let the reaction occur for 30, 60, 120, and 300 seconds. Allowing the reaction to occur for longer than 30 seconds did not show any statistically significant change in λ_{max} from the 30-second time point (Figure S2 of supporting information). From these results, we have shown that the reaction time did not influence the λ_{max} of the nanostars.

The standard deviation of all the time trials at 5 °C was about ± 14 nm (n = 12). This was still statistically smaller (F-Test, $\alpha = 0.05$) than the ± 39 nm (n = 4) standard deviation of the reaction at 25 °C. Thus, not only did the temperature-mediated method yield reproducible nanostars, but the nanostars were also reproducible across different reaction times. The average λ_{max} for all reaction times was 708 nm, about 40 nm lower than expected. The reason for this had to do with the stability of the gold chloride and not the reaction temperature. The shifts in plasmon λ_{max} will be elaborated on in the following sections.

Concentration Matching Gold Nanostar Samples

While the λ_{max} was found to be reproducible in gold nanostars synthesized at 5 °C, the raw intensity of the optical density was not always consistent. Using a Nanosight instrument, we were able to obtain an approximate concentration of the nanostars to prepare concentration matched solutions for analysis of the optical density and extinction coefficients of the nanostars plasmon bands. The reader should note that the Nanosight concentration estimates are approximate values, and these values are not the most accurate. Atomic emission or other similar methods will give a more accurate estimate of the concentrations. However, provided the instrument acquisition settings remain unchanged for analysis of different samples, the Nanosight is precise enough to compare the relative concentrations of each synthesis trial used in the concentration matching experiments.

Nanostars were synthesized at 5 and 25 °C in triplicate at each temperature. Figure S3 in the supporting information shows the concentration matched plasmon bands of gold nanostars for both 25 °C (Figure S3a) and 5 °C (Figure S3b). Prior to dilution of the nanostars synthesized at 5 °C, the peak optical density values were 2.554, 2.798, and 2.728. This gave an average of 2.693 with a standard deviation of ± 0.126. Using the Nanosight data, we were able to approximately match the concentrations to 1.25×10^{11} nanostars/mL. The optical densities of concentration matched nanostars were 2.358, 2.540, and 2.395. The average optical density was 2.431 ± 0.096.

For the synthesis at 25 °C, the optical densities were 2.882, 1.768, and 2.046. This gave an average optical density of 2.232 with a standard deviation of ± 0.580 prior to concentration matching. After matching the concentrations to 4.74×10^{10} nanostars/mL, the optical densities

were 2.031, 1.629, and 1.894 giving an average optical density 1.851 ± 0.204. Although the optical densities can vary after initial synthesis at both temperatures, we have demonstrated the ability to control the concentration of these nanoparticles in solution after their initial synthesis.

Extinction coefficients are wavelength dependent but not concentration dependent. Since the Nanosight and UV/Vis acquisition settings were the same for nanostars made at both temperatures, a statistical comparison of the extinction coefficients was possible. Six solutions were analyzed at each temperature (three unmatched and three matched concentrations). Comparison of the extinction coefficients between the different nanostar solutions must be done at the same λ_{max}. For each temperature investigated, the extinction coefficient was determined for each solution, resulting in six extinction coefficients at each of the six λ_{max} values. There was no statistical difference ($\alpha = 0.05$, n = 6) between the extinction coefficients of the unmatched and matched concentration solutions at each of the six λ_{max} values for either of the temperatures investigated. This result was expected as the extinction coefficient is independent of the concentration. Furthermore, the extinction coefficients could be used, cautiously, to estimate nanostar concentration based on optical density at a given wavelength.

At each λ_{max} value the extinction coefficients of the matched and unmatched concentrations were pooled to find the average extinction coefficients for the 5 and 25 °C nanostars. The average extinction coefficients for the 5 °C nanostars ranged from 1.932 ± 0.194 x 10^{-11} $\frac{cm^2}{particle}$ (10. % RSD) at 748 nm to 1.995 ± 0.113 x 10^{-11} $\frac{cm^2}{particle}$ (5.7 % RSD) at 718 nm (n = 6). The average extinction coefficients for the 25 °C nanostars ranged from 3.765 ± 0.306 x 10^{-11} $\frac{cm^2}{particle}$ (8.1 % RSD) at 930 nm to 3.811 ± 0.353 x 10^{-11} $\frac{cm^2}{particle}$ (9.3 % RSD) at 898 nm (n = 6).

To compare the average extinction coefficients, the 720 nm plasmon wavelength was chosen because it fell within the plasmon bands of both the 5 and 25 °C nanostars. The average extinction coefficients for the 5 and 25 °C nanostars were 1.995 ± 0.119 x 10^{-11} $\frac{cm^2}{particle}$ (5.9 % RSD) and 2.341 ± 0.276 x 10^{-11} $\frac{cm^2}{particle}$ (12 % RSD), respectively (n = 6). The average extinction coefficients at 5 and 25 °C were statistically different (α = 0.05). The difference in the average extinction coefficients at 720 nm for the 5 and 25 °C nanostars indicates that there were fundamental differences in the geometric and plasmonic properties of the nanostars made at the two temperatures. Similar comparisons and results were made for the average extinction coefficient at each λ_{max} value, but the confidence level varied from α = 0.001 to α = 0.10 (data not shown).

Since the extinction coefficient is wavelength dependent the average extinction coefficients from each λ_{max} could not be averaged together to get a standard deviation. Instead the standard deviation of the extinction coefficient at each λ_{max} value was averaged to compare average standard deviations between 5 and 25 °C. The average standard deviation of the extinction coefficient was shown to be statistically smaller (α = 0.05, n = 6) for the nanostars synthesized at 5 °C compared to nanostars synthesized at 25 °C. This provides additional support that nanostars synthesized at 5 °C were more reproducible. Both the 5 and 25 °C synthesis showed average λ_{max} values about 40 and 70 nm, respectively, away from those previously discussed. The reason for this shift in wavelength will be discussed in detail below.

Proper Reagent Care and the Influence on Synthesis

While synthesizing biocompatible gold nanostars at 5 °C, we found it essential to take great care of the gold chloride. It must be kept in a very dry environment and protected from air to

prevent the gold from being reduced or further hydrated. We found that if the gold chloride was in use for several months, or left out of the desiccator, then the nanostar plasmon bands were blue shifted relative to nanostars synthesized with a previously unopened bottle of gold chloride. While the plasmon band exhibited a shift, the gold nanostars made at 5 °C were still reproducible at the new λ_{max} (Figure S2). We suspect this shift to be a result of trace reducing agents in the air reacting with water and gold to alter the oxidation state of the gold prior to use for synthesis. The gold chloride, when left outside a desiccator or even left in solution, will influence the nanostar synthesis. We recommend using the gold chloride solution immediately after its preparation. If proper care is kept of the gold chloride, then gold nanostars with a reproducible λ_{max} will continue to be produced. For care of the solid gold chloride, we recommend sealing the lid with parafilm wax to protect from reducing agents in the air, wrapping tin foil around the bottle to protect from light, and placing the bottle in a desiccator to protect from water.

Validation of Nanostar Plasmon Reproducibility from Synthesis at 5 °C

Throughout this work, the plasmon λ_{max} values shifted for syntheses at both 5 and 25 °C. For each temperature, plasmon UV/Vis data from the nanostars made by each author, JR and LZ, were pooled to validate that the 5 °C synthesis actually produced more reproducible plasmon bands than those made at 25 °C. In doing so we found the average plasmon λ_{max} was 718.4 ± 26.6 nm (n = 27) and 818.9 ± 68.5 nm (n = 15) for the 5 and 25 °C, respectively. From an F-test ($\alpha = 0.05$) the standard deviation from synthesis at 5 °C was statistically smaller and thus more reproducible.

Figure 7 shows a box and whisker plot of the pooled nanostar data for synthesis at 5 and 25 °C. These plots show the broad range of values for λ_{max} for nanostars made at 25 °C compared to 5 °C. The λ_{max} values for nanostars synthesized at 25 °C span almost 150 nm compared to about

50 nm for nanostars synthesized at 5 °C. The tighter distribution of data in the 5 °C nanostars showed a higher degree of reproducibility than was achieved with the broad ranging 25 °C nanostars.

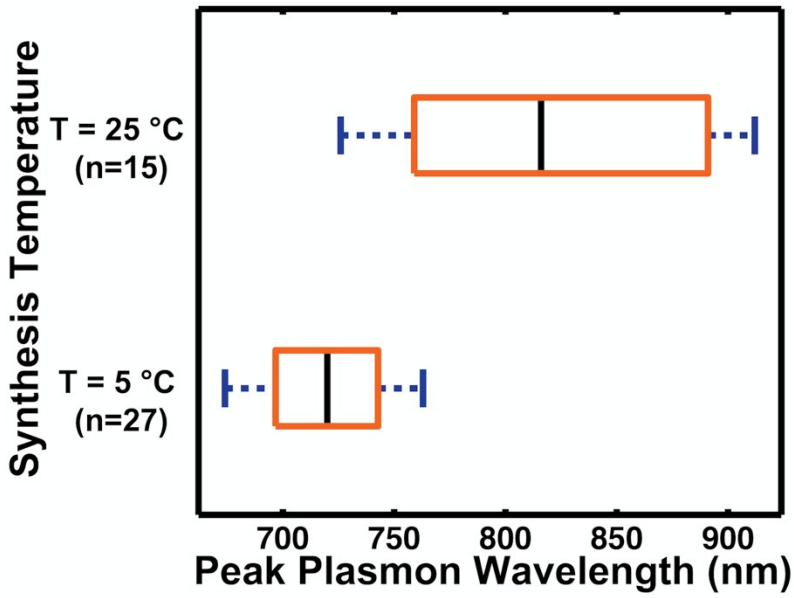

Figure 7. Box and Whisker plot of pooled nanostar plasmon data from authors JR and LZ to compare plasmon λ_{max} reproducibility of the synthesis at 5 °C, n = 27 and 25 °C, n = 15. Pooling the data from each author helped validate that the 5 °C nanostar synthesis gave more reproducible peak plasmon wavelengths than the synthesis at 25 °C.

CONCLUSION

In conclusion, a method for 5 °C temperature/seed-mediated synthesis of biocompatible gold nanostars with reproducible plasmon bands and spectral widths has been presented. The novelty of the temperature-mediated synthesis lies in the reproducibility of the spectral response. Another novelty of the approach is the use of temperature to tune the plasmon band in addition to changing the $AgNO_3$ concentration. The low temperature nanostar synthesis kept the

plasmons in the NIR region making the nanostars ideal for bioanalytical and other biological applications.

A lower standard deviation in the λ_{max} corresponded to greater reproducibility of the spectral response from the nanostars. While synthesis at 25 °C produced nanostars with λ_{max} values in the NIR region, it could not do so in a reproducible manner. The standard deviation of the plasmon λ_{max} values from synthesis at 5 °C under two different $AgNO_3$ concentrations was found to be statistically smaller than those of the synthesis at 25 °C. While the plasmon band varied depending on the age of the gold chloride and the person making the nanostars at both 5 and 25 °C, on average the 5 °C synthesis proved more reproducible.

We suspect the reproducible plasmon peaks were the result of altered reaction conditions at 5 °C that provided more control over the synthesis to produce, on average, a more homogenous distribution of nanostars with more reproducible spike characteristics. Future studies are planned to elucidate the nature of the reproducibility and study the synthetic mechanism to understand how the synthesis changed at 5 °C. We also plan to use the reproducible/tunable gold nanostars in the future for sensitive and reproducible Surface Enhanced (Resonant) Raman Scattering biosensors.

Acknowledgements

Conflict of Interest: The authors declare no competing financial interest.

The authors acknowledge Oregon State University for support of this research. Especially from the Research Office General Research Grant.

(The Oregon State University Electron Microscopy Suite)

The electron microscopy facility used to acquire TEM images is supported by the National Science Foundation via the Major Research Instrumentation (MRI) Program under Grant No. 1040588. We also gratefully acknowledge financial support for the acquisition of the TEM instrument from the Murdock Charitable Trust and the Oregon Nanoscience and Microtechnologies Institute (ONAMI).

We would like to thank and extend our great appreciation to the Koley Group (Oregon State University) for the use of their UV/Vis spectrophotometer. In addition, we would like to thank the Harper Group (Oregon State University) for the use of their Nanosight instrument.

Notes and references

† Supporting Information: Reaction Time Study, Changing Silver Concentration, Concentration Matching, Altered Gold Chloride Reproducibility

Corresponding Author

*sean.burrows@oregonstate.edu

Present Addresses

[a] Department of Chemistry, Oregon State University, Corvallis, Oregon 97331, United States of America

[b] Department of Biology, Tufts University, Medford MA 02155, United States of America.

Author Contributions

The manuscript was written through contributions of all authors. All authors have given approval to the final version of the manuscript.

Funding Sources

We would like to thank Oregon State University and the Research Office General Research Grant for supporting this work. C. Kyle Almlie would like to thank the Milton Harris Graduate Fellowship for summer support toward this project.

ABBREVIATIONS

DI, Deionized water; LSPR, local surface plasmon resonance; μm, micrometer; NIR, Near Infrared; nm, nanometer; RSD, relative standard deviation; SERS, Surface Enhanced Raman Scattering; SERRS, Surface Enhanced Resonant Raman Scattering; UV, ultraviolet; Vis, visible.

REFERENCES

1 H. Yuan, C. G. Khoury, H. Hwang, C. M. Wilson, G. A. Grant and T. Vo-Dinh, *Nanotechnology*, 2012, **23**, 075102.

2 R. Alvarez-Puebla, L. M. Liz-Marzán and F. J. García de Abajo, *J. Phys. Chem. Lett.*, 2010, **1**, 2428–2434.

3 O. Bibikova, A. Popov, I. Skovorodkin, A. Prilepskyi, T. Pylaev, A. Bykov, S. Staroverov, V. Bogatyrev, V. Tuchin, M. Kinnunen, S. Vainio, K. Kordas and N. Khlebtsov, 2013, vol. 8801, pp. 880102–880102–8.

4 S. K. Dondapati, T. K. Sau, C. Hrelescu, T. A. Klar, F. D. Stefani and J. Feldmann, *ACS Nano*, 2010, **4**, 6318–6322.

5 L. Rodríguez-Lorenzo, R. A. Álvarez-Puebla, F. J. G. de Abajo and L. M. Liz-Marzán, *J. Phys. Chem. C*, 2010, **114**, 7336–7340.

6 S. Barbosa, A. Agrawal, L. Rodríguez-Lorenzo, I. Pastoriza-Santos, R. A. Alvarez-Puebla, A. Kornowski, H. Weller and L. M. Liz-Marzán, *Langmuir*, 2010, **26**, 14943–14950.

7 L. Shao, A. S. Susha, L. S. Cheung, T. K. Sau, A. L. Rogach and J. Wang, *Langmuir*, 2012, **28**, 8979–8984.

8 C. Hrelescu, T. K. Sau, A. L. Rogach, F. Jäckel, G. Laurent, L. Douillard and F. Charra, *Nano Lett.*, 2011, **11**, 402–407.

9 F. Hao, C. L. Nehl, J. H. Hafner and P. Nordlander, *Nano Lett.*, 2007, **7**, 729–732.

10 E. S. Allgeyer, A. Pongan, M. Browne and M. D. Mason, *Nano Lett.*, 2009, **9**, 3816–3819.

11 C. G. Khoury and T. Vo-Dinh, *J. Phys. Chem. C*, 2008, **112**, 18849–18859.

12 A. S. Thakor, J. Jokerst, C. Zavaleta, T. F. Massoud and S. S. Gambhir, *Nano Lett.*, 2011, **11**, 4029–4036.

13 A. M. Fales, H. Yuan and T. Vo-Dinh, *J. Phys. Chem. C*, 2014, **118**, 3708–3715.

14 H. Yuan, A. M. Fales, C. G. Khoury, J. Liu and T. Vo-Dinh, *J. Raman Spectrosc.*, 2013, **44**, 234–239.

15 S. C. Glotzer and M. J. Solomon, *Nat. Mater.*, 2007, **6**, 557–562.

16 H.-L. Wu, H.-R. Tsai, Y.-T. Hung, K.-U. Lao, C.-W. Liao, P.-J. Chung, J.-S. Huang, I.-C. Chen and M. H. Huang, *Inorg. Chem.*, 2011, **50**, 8106–8111.

17 M. Li, J. Zhang, S. Suri, L. J. Sooter, D. Ma and N. Wu, *Anal. Chem.*, 2012, **84**, 2837–2842.

18 B. L. Sanchez-Gaytan, Z. Qian, S. P. Hastings, M. L. Reca, Z. Fakhraai and S.-J. Park, *J. Phys. Chem. C*, 2013, **117**, 8916–8923.

19 D.-K. Lim, K.-S. Jeon, J.-H. Hwang, H. Kim, S. Kwon, Y. D. Suh and J.-M. Nam, *Nat. Nanotechnol.*, 2011, **6**, 452–460.

20 S. P. Hastings, P. Swanglap, Z. Qian, Y. Fang, S.-J. Park, S. Link, N. Engheta and Z. Fakhraai, *ACS Nano*, 2014, **8**, 9025–9034.

21 J. Xie, J. Y. Lee and D. I. C. Wang, *Chem. Mater.*, 2007, **19**, 2823–2830.

22 X.-L. Liu, J.-H. Wang, S. Liang, D.-J. Yang, F. Nan, S.-J. Ding, L. Zhou, Z.-H. Hao and Q.-Q. Wang, *J. Phys. Chem. C*, 2014, **118**, 9659–9664.

23 P. S. Kumar, I. Pastoriza-Santos, B. Rodríguez-González, F. J. G. de Abajo and L. M. Liz-Marzán, *Nanotechnology*, 2008, **19**, 015606.

24 A. Topete, M. Alatorre-Meda, E. M. Villar-Álvarez, A. Cambón, S. Barbosa, P. Taboada and V. Mosquera, *ACS Appl. Mater. Interfaces*, 2014, **6**, 11142–11157.

25 R. Sardar, A. M. Funston, P. Mulvaney and R. W. Murray, *Langmuir ACS J. Surf. Colloids*, 2009, **25**, 13840–13851.

26 A. J. Mieszawska, W. J. M. Mulder, Z. A. Fayad and D. P. Cormode, *Mol. Pharm.*, 2013, **10**, 831–847.

27 A. Casu, E. Cabrini, A. Donà, A. Falqui, Y. Diaz-Fernandez, C. Milanese, A. Taglietti and P. Pallavicini, *Chem. – Eur. J.*, 2012, **18**, 9381–9390.

28 P. Pallavicini, G. Chirico, M. Collini, G. Dacarro, A. Donà, L. D'Alfonso, A. Falqui, Y. Diaz-Fernandez, S. Freddi, B. Garofalo, A. Genovese, L. Sironi and A. Taglietti, *Chem. Commun.*, 2011, **47**, 1315–1317.

29 P. Pallavicini, A. Donà, A. Casu, G. Chirico, M. Collini, G. Dacarro, A. Falqui, C. Milanese, L. Sironi and A. Taglietti, *Chem. Commun.*, 2013, **49**, 6265–6267.

30 G. Cavallaro, D. Triolo, M. Licciardi, G. Giammona, G. Chirico, L. Sironi, G. Dacarro, A. Donà, C. Milanese and P. Pallavicini, *Biomacromolecules*, 2013, **14**, 4260–4270.

31 P. Dey, I. Blakey, K. J. Thurecht and P. M. Fredericks, *Langmuir*, 2013, **29**, 525–533.

32 J. R. G. Navarro, A. Liotta, A.-C. Faure, F. Lerouge, F. Chaput, G. Micouin, P. L. Baldeck and S. Parola, *Langmuir*, 2013, **29**, 10915–10921.

33 H. Yuan, Y. Liu, A. M. Fales, Y. L. Li, J. Liu and T. Vo-Dinh, *Anal. Chem.*, 2013, **85**, 208–212.

34 W. Callister, *Materials Science and Engineering An Introduction, (Pages 312-320)*, John Wiley & Sons, Inc., Seventh., 2007.

35 R. Lévy, N. T. K. Thanh, R. C. Doty, I. Hussain, R. J. Nichols, D. J. Schiffrin, M. Brust and D. G. Fernig, *J. Am. Chem. Soc.*, 2004, **126**, 10076–10084.

Table of Content Figure:

The novelty and significance lies in the low temperature synthesis to improve reproducibility of the plasmonic response by a factor of at least two compared to current approaches.